Synthesis of Large-Pore Micelle-Templated Silico-Aluminas at Different Alumina Contents

Anne Galarneau,‡ Michela Cangiotti,† Francesco di Renzo,‡ Federica Sartori,† and M. Francesca Ottaviani*,†

Institute of Chemical Sciences, University of Urbino, Piazza Rinascimento 6, 61029 Urbino, Italy, and Laboratoire de Matériaux Catalytiques et Catalyze en Chimie Organique, UMR 5618 ENSCM-CNRS, 8 Rue de l'Ecole Normale, Institut Gerhardt FR 1878, 34296 Montpellier Cedex 5, France

Received: July 3, 2006; In Final Form: August 10, 2006

The EPR spectra of radical surfactant probes embedded in cetyltrimethylammonium bromide (CTAB) and trimethylbenzene (TMB) stable water emulsions (TMB/CTAB = 13) were analyzed to provide information on the kinetics of formation of micelle-templated silicoaluminas (MTSA) at 343 K, obtained by means of silica and alumina, solved in alkaline solutions, at different Si/Al ratios. Textural (surface area, pore volume, pore size, surfactant content) and structural characterization of both as-synthesized and calcined MTSA were performed by means of nitrogen sorption isotherms, TEM, and chemical analysis. This analysis showed that TMB worked as a swelling agent of the CTAB micelles, providing large-pore homogeneous and stable MTSA at TMB/CTAB = 13 for Si/Al from ∞ to 10. A demixing of the emulsion occurs at Si/Al < 10: at Si/Al = 7, a double wide-and-narrow pore structure was formed; then, at Si/Al = 5, an amorphous material was obtained. At Si/Al ≥ 10, the computer-aided analysis of the EPR spectra as a function of the synthesis time indicated the distribution of the probes in two different environments: "micellar" probes inserted in the surfactant aggregates, whose mobility decreases over the synthesis time, thus reporting on the progressive modification of the surfactant aggregates structure and the solid condensation, and "interacting" probes due to probe−surfactant heads electrostatically interacting with the charged surface sites induced by alumina incorporation in the silica network. This last fraction increases its relative amount over the synthesis time, informing about the condensation and structuration of the MTSA. Without alumina, the "interacting" component is absent in the EPR spectra because TMB preferentially interacts with the surfactant headgroups by cation−π interactions, thus preventing the interactions of these headgroups with silanols. When alumina is added, the negatively charged silicoaluminate at the surface promotes the interaction of the ammonium headgroups with the surface, and some Na^+ cations also interact with TMB by cation−π interaction and contribute to decreasing the interaction of the headgroups with TMB. Therefore, increasing alumina contents promote electrostatic interactions between the positively charged surfactant heads and the negatively charged silicoaluminate groups. The strong interaction of the surfactants with the silicoaluminate surface allows the formation of a monolayerlike structure of surfactant, which is not observed in the absence of alumina. The synthesis is slowed by increasing alumina contents due to a destructuration effect of alumina in the MTSA formation.

Introduction

The innovative homoporous solids, which are built from a cooperative assembly of micelles and silicates, are accordingly termed micelle-templated silica (MTS).[1−6] The micelles generate mesopores with a size in the range between 20 and 150 Å, providing high and selective adsorption of guest molecules. Therefore, this material shows applications in physicochemical fields such as catalysis, adsorption, and host−guest chemistry.[7−13] Micelles constituted by cetyltrimethylammonium bromide (CTAB) as surfactant form a stable hexagonal structure featuring a pore size of 37 Å.[14,15] To precipitate and polymerize the solid over the micelles, two different sources of silica have been used:[16−23] tetraethoxysilane (TEOS), which leads to a synthesis controlled by hydrolysis of the reactants, and solid silica (SiO_2) solved in a alkaline solution, which leads to a synthesis controlled by the material organization.

EPR, combined with XRD and sorption isotherms, has been shown to be a powerful tool to clarify the mechanism of MTS formation.[24−30] Radical surfactants have been dissolved in the micelles and work as probes to get information of the MTS synthesis. Using TEOS, Goldfarb and co-workers have found a fast formation of hexagonal MTS in the first 12−13 min of synthesis, followed by a slow reorganization of the solid.[24,25] Conversely, dissolved silica initially forms a metastable disordered precursor, followed by a slow formation of the final hexagonal MTS.[26] The formation of hexagonal micelle-templated silicoalumina (MTSA) obtained with alkyltrimethylammonium bromide of different chain lengths (*n*TAB, *n* = 8−18) and Si/Al = 30 follows an equivalent kinetics.[27] The longer the alkyl chain, the faster the MTS formation and the higher the number of surfactant strongly interacting with the silica due to the resulting larger pore size. Strongly interacting and poorly interacting surfactants were located at the sides and at the corners of the hexagonal pores, respectively, corresponding to hydrophilic (silanols and aluminate) and hydrophobic (siloxane) parts of the pore, respectively. More recently,[28] large-pore MTS (pore

* Corresponding author. E-mail: ottaviani@uniurb.it. Telephone: +39−0722−303319. Fax: +39−0722−303311.

† Institute of Chemical Sciences, University of Urbino.

‡ Laboratoire de Matériaux Catalytiques et Catalyze en Chimie Organique.

10.1021/jp064156i CCC: $33.50
Published on Web 09/13/2006

size > 50 Å) with high surface area (900 m^2/g) were studied by EPR analysis. Large-pore MTS were obtained by adding 1,3,5-trimethylbenzene (TMB) to the CTAB micelles in order to increase the pore size of MTS. It was found that an "intermediate" TMB content (TMB/CTAB = 5) provided two-sized porosities, described by the demixing of the emulsion formed by the TMB−CTAB−water mixture; whereas at high TMB content (TMB/CTAB = 13), a stable emulsion gave rise to one-sized pores (110 Å). The kinetic at TMB/CTAB = 13 was faster compared to MTS synthesis without TMB due to the surface formation of low polar siloxane sites in vicinity of TMB molecules. Therefore, TMB promotes the silanol condensation to form low polar siloxane groups at the pore sides and consequently enhances the hydrophobicity due to the location of the hydrophobic TMB in vicinity of the surfactant heads.[29] Very recently, the synthesis of "unswelled" (without TMB) MTSA has been analyzed by EPR by changing the Si/Al ratio.[30] It has been found that the increase in the alumina content slows down the kinetics of the synthesis and promotes the interactions between the surfactant heads and the surface due to the presence of silicoaluminate groups at the pore sides. Electrostatic interactions between the surfactant heads and the negatively charged surface groups increases from 35 to 60% for MTS using a Si/Al ratio from ∞ to 30, respectively, and remains constant until Si/Al = 15. At higher alumina contents (Si/Al < 15), the structuration of the hexagonal solid is impeded by the formation of an amorphous silicoaluminate solid, which contributes to decreasing the surface area and the pore volume of the materials.[30]

In the present study, the kinetics of formation of large-pore MTSA (TMB/CTAB = 13) at different Si/Al ratios were followed by analyzing the modifications of the EPR spectra over time for the probe 4-cetyldimethylammonium-2,2,6,6-tetramethyl-piperidine-*N*-oxide bromide (CAT16), embedded into the TMB−CTAB microemulsion. The EPR spectra were mainly analyzed by the computation of the EPR line shape, extracting structural, mobility, and polarity parameters indicative of the modifications of the surfactant aggregates and the solid over time. The CAT16 probe was selected because it resulted, from previous studies,[24−28,30] as the most informative to report about the structuration of the solid over time. This is because the nitroxide group localizes at the aggregate surface and reports on the condensation process of the solid. The 5-doxylstearic (5DSA) probe was also used: the nitroxide group of 5DSA localized in the lipid core of the aggregates, in vicinity of the head layer. The EPR spectrum of 5DSA poorly modified over time and only indicated that the structure of the aggregates is well packed and organized from the first minutes of the synthesis, independently of the Si/Al ratio. Therefore, the results of this probe are not informative about the different kinetics of synthesis of the large-pore MTSA and are not henceforth discussed in this paper.

The synthesis was performed at 343 K; this temperature guarantees, on the basis of the solid characterization, obtaining homogeneous and reproducible homomesoporous solids. The alumina contents, measured as Si/Al, ranged from ∞ (correspondent to pure silica) to 5.

Nitrogen sorption isotherms at 77 K, transition electron microscopy (TEM), thermogravimetric analysis, and chemical analysis were carried out to characterize both as-synthesized and calcined MTSA materials. As already found in previous studies,[28,29] XRD could not be used for the solid characterization in case the pores are too large to correctly determine the cell parameters.

This study shows how the formation process of large-pore MTSA, as well as the nature of the solid surface, formed by means of a stable TMB−CTAB emulsion, is modified by varying the Si/Al ratio.

Experimental Section

Materials. The Al−MTS mesostructures (named MTSA) were synthesized by using cetyltrimethylammonium bromide (CTAB, Aldrich) as a surfactant, fumed silica (Aerosil 200, Degussa) as a source of silica, $NaAlO_2$ (Aldrich) as a source of alumina, NaOH as an alkaline source, and 1,3,5-trimethylbenzene (TMB, Aldrich) as a micelle swelling agent, and Millipore double-distilled water. For the synthesis studied by EPR, 4-cetyldimethylammonium-2,2,6,6-tetramethyl-piperidine-*N*-oxide bromide (CAT16), kindly provided by Dr. Xuegong Lei, Columbia University, New York, USA, was used as a spin probe.

Synthesis for MTSA Characterization. The molar ratios of the components in the synthesis were: $1SiO_2/0-1NaAlO_2$ (to obtain Si/Al = ∞, 60, 30, 15, 10, 7, 6, 5)/0.25NaOH/0.1 CTAB/1.3 TMB/$20H_2O$. A first solution of CTAB and TMB in alkaline solution (NaOH) mixed with $NaAlO_2$ was prepared and stirred at 298 K in a stainless steel autoclave. SiO_2 was then added to this solution under stirring to give gel mixtures at the different Si/Al ratios. After 30 min of stirring at 298 K, the autoclave was sealed and heated at 343 K for 24 h under static conditions (we also performed synthesis at higher temperatures: from 343 to 388 K, the obtained solids presented an equivalent structure, on the basis of the solid characterization, but the higher the temperature, the faster the synthesis). The solid precipitate was then recovered by filtration, washed with water, and then dried at 353 K overnight to obtain the so-called as-synthesized MTSA. Calcination of as-synthesized MTSA was performed at 823 K for 8 h under air flow to remove the organic matter (surfactants) and therefore to obtain the so-called calcined MTSA.

Synthesis of MTSA in the EPR Cavity. The molar ratios of the components in the synthesis were: $1SiO_2/0-1NaAlO_2$ (to obtain Si/Al = ∞, 60, 45, 30, 20, 15, 10, 7, 5)/0.25NaOH/0.1 CTAB/1.3 TMB/0.0001 CAT16/$20H_2O$. The spin probe CAT16 was first added to the CTAB micelle solution in water and left equilibrating for 1 day. Then the other synthesis components were added under stirring at 298 K in the sequence: TMB, NaOH, $NaAlO_2$, and SiO_2 at the different Si/Al ratios. Before and after addition of TMB, 20 μl aliquots were transferred in EPR tubes to obtain reference EPR spectra. The final gel mixtures of MTSA were stirred at 298 K for 30 min. Then each synthesis mixture was immediately inserted in a tube; this tube was sealed and fixed into the EPR cavity equilibrated at 343 K. EPR spectra were recorded at subsequent synthesis times ($t = 0$ corresponded to the insertion time into the EPR cavity; the time needed for the tuning of the cavity and equilibration of the temperature in the sample was 1 min). The synthesis was monitored by computer analysis of the EPR spectra of CAT16 embedded in the CTAB + TMB aggregates.

Computation of the EPR Spectra. The analysis of the EPR spectra was performed by means of the well-established procedure of Budil and Freed,[31] obtained by using, as main parameters, the perpendicular component of the correlation time for motion, τ_{perp} (a Brownian model for the diffusional motion was assumed), and when necessary, the order parameter S (ranging from $S = 0$, that is, no order, to $S = 1$, for complete ordering). Both the g_{ii} components, for the coupling between the electron spin and the magnetic field, and the A_{ii} components,

TABLE 1: Main Properties of MTSA, at Different Si/Al Ratios, Obtained from Swelled CTAB Micelles: Si/Al, Na/Al, CTAB/Al Contents in the As-Synthesized Materials[a]

Si/Al (gel)	Si/Al (as-synthesized)	Na/Al (as-synthesized)	CTAB/Al	Na/Al exchanged with NH_4^+	CTAB yield (%)	SiO_2 yield (%)	S (m^2/g)	V (mL/g)	D (Å)
∞	1326	0	0	0	96	50	843	2.01	104
60	74	0.5	8.8	0.05	96	81	987	1.90	87
30	39	0.3	5.5	0.03	98	70	980	1.79	76
15	15	0.3	2.1	0.04	98	70	893	1.55	81
10	10	0.3	1.1	0.07	76	71	826	1.76	96
7	7	0.6	0.8	0.21	80	74	679	0.91	35+92
6	3	0.7	0.1	0.35	41	100	618	0.60	35
5	5	0.7	0.3	0.34	71	85	479	0.75	100

[a] Molar yields (in %) of SiO_2 and CTAB incorporated in the as-synthesized materials; specific surface area (S), pore volume (V), and pore diameter (D) obtained from nitrogen sorption isotherms of calcined MTSA.

for the coupling between the electron spin and the nitrogen nuclear spin, were taken constant ($g_{ii} = 2.009, 2.006, 2.002$; $A_{ii} = 7, 7, 33$ G): their variations were negligible from one another of these similar systems, as obtained from the frozen solutions. The A_{ii} values indicate an environment of middle polarity, as expected for CAT16 in surfactant aggregates in a water solution or at a polar surface.

The increase in τ_{perp} reports for the slowing down of the rotational mobility of the probe due to the increased environmental viscosity and/or the interactions between the radical−surfactant heads and the solid surface; the order parameter reports on the formation of a layerlike structure of surfactants.

Finally, if two or more components contribute to the overall EPR signal, the subtraction of spectra recorded in different experimental conditions (for instance, the different Si/Al ratios) allows extraction of the single components and computation of each of them. The double integration of the subtracted components provides the relative percentages of the components, correspondent to the percentages of probes in different environments. Addition of the computed spectral components at the obtained relative percentages leads to reproduction of the experimental line shape.

The accuracy of the EPR parameters is between 2 and 5%, depending on spectral resolution and on the fitting between the experimental spectrum and the computed spectrum.

Instrumentation. The EPR spectra were recorded by means of a EMX-Bruker spectrometer operating at X band (9.5 GHz) and interfaced to a IBM PC computer (Bruker software) for data acquisition and handling. The temperature was controlled with a Bruker ST3000 variable-temperature assembly. The spectra were considered valid only on condition of reproducibility of the spectral line shape for different samples of the same materials in the same experimental conditions.

The adsorption/desorption isotherms at 77 K of the MTSA materials were measured using a Micromeritics ASAP 2010 instrument. The calcined samples were outgassed at 523 K until a stable static vacuum of 3×10^{-3} Torr was reached. The mesopore diameter was calculated from the desorption branch of nitrogen isotherms by Broekhoff and de Boer (BdB) method,[32] which has been shown to provide reliable results for MCM-41 materials.[33] Special care was taken in the determination of the BET specific surface area to calculate the linearization of the BET equation: both the lowest and the highest pressure values were neglected because they were affected by the surface heterogeneity and by the initial pore filling, respectively. Pore volumes were calculated at the end of the step corresponding to the pore filling.

Transmission electron microscopy (TEM) was performed using a Philips CM30T electron microscope with an LaB6 filament at 300 kV. Samples were mounted on a microgrid carbon polymer supported by a copper grid. A few droplets of a suspension of ground sample in ethanol were dropped on the grid and then dried at ambient conditions.

Thermogravimetric analysis (TGA) was performed using a Netzsch TG209C balance. The heat rate was maintained at 5°C/min in air flow up to 1123 K. CTMA and SiO_2 yields (in mol %) of the synthesis were determined from TGA and were = [(amount of element in the as-synthesized dried solid)/(total amount of element in the gel)] × 100 (Table 1).

Chemical Analysis. Al and Na contents in as-synthesized materials were determined by chemical analysis by the CNRS center of analysis at Vernaizon (France) (Table 1). To verify the accessibility of Na^+ cations in calcined MTSA material, cation exchange Na^+/NH_4^+ was performed, as described in the following, giving rise to acidic material, H^+−MTSA. Calcined MTSA materials (1 g) were equilibrated in 100 mL $(NH_4)NO_3$ (0.1 M) in EtOH. The treatment was repeated three times. The samples were finally calcined at 723 K for 6 h. Na content in H^+−MTSA materials was determined by chemical analysis. The remaining amount of Na^+ is reported in Table 1.

Results and Discussion

MTSA Characterization. MTSA syntheses were performed with a large excess of TMB (TMB/CTAB = 13) to promote the formation of homogeneous materials with large pore diameter (D) (∼100 Å), narrow pore size distribution, large pore volume (V) (∼2 mL/g), and high surface area (S) (∼900 m^2/g), as resulted from previous studies for large-pore MTS (in the absence of alumina).[28,29] Figure 1a shows, as examples, the nitrogen adsorption/desorption isotherms at 77 K of calcined large-pore MTSA obtained with TMB/CTAB = 13 at Si/Al (in the gel synthesis) = ∞, 30, and 10.

The analysis of the isotherms provided the pore diameters, the pore volumes, and the surface areas of MTSA at the different Si/Al ratios reported in Table 1. Large-pore MTSA obtained from Si/Al from ∞ to 10 features average values of $V = 1.8$ mL/g, $D = 90$ Å, and $S = 900$ m^2/g (Table 1), but the observed changes are interesting and informative on the structure variations.

From Si/Al = ∞ to Si/Al = 60, the surface area increased from 843 to 987 m^2/g, the pore volume slightly decreased from 2.0 to 1.9 mL/g, and the pore diameter decreased from 104 to 87 Å. This means that the texture of MTS was significantly modified by adding a relatively small amount of alumina due to a decreasing swelling effect of TMB. To control how this texture variation affected the wall-thickness of the pores, we calculated this value by means of the following equation:[34]

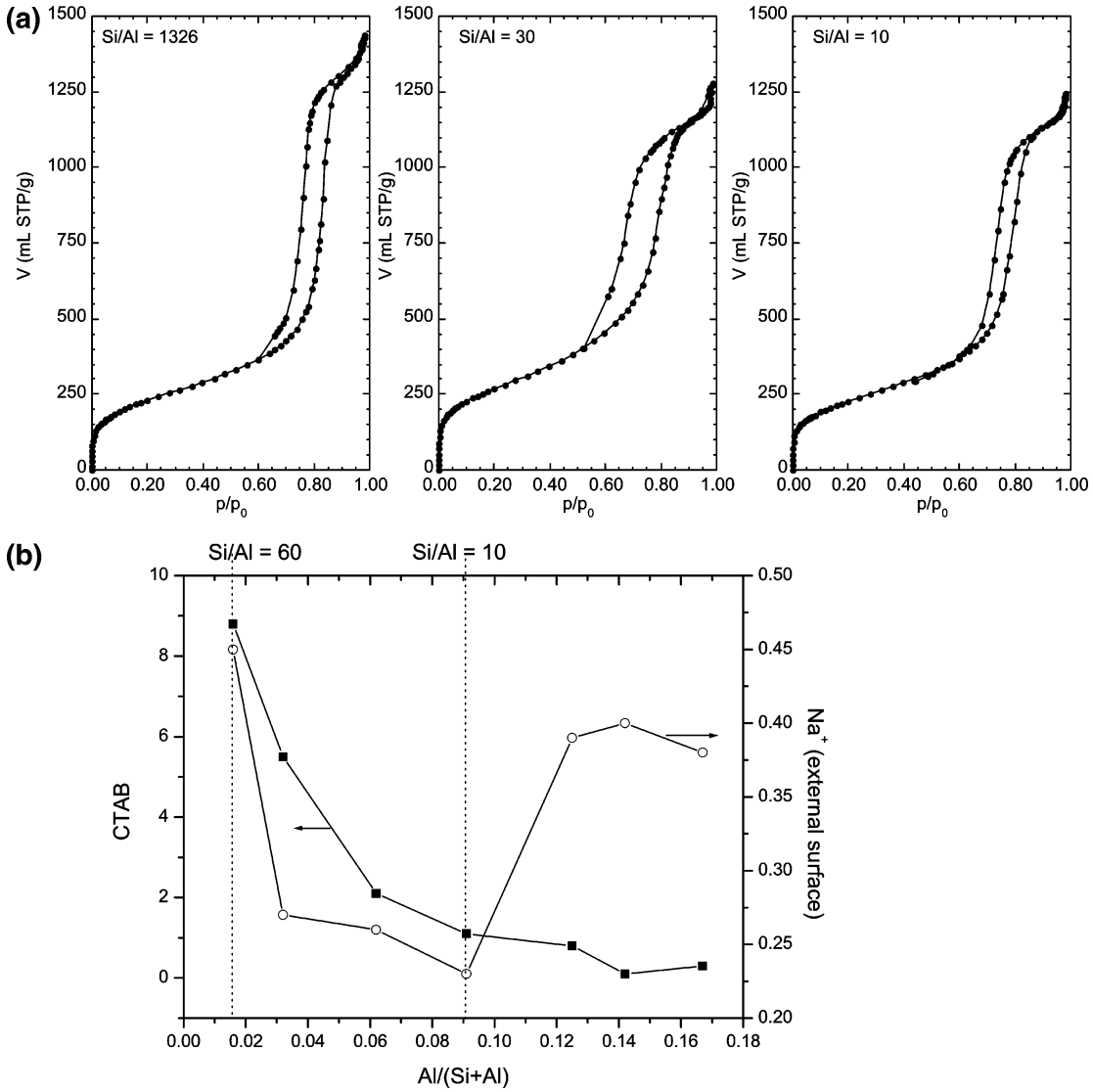

Figure 1. (a) Adsorption/desorption isotherms at 77 K of calcined MTSA obtained with TMB/CTAB = 13 at Si/Al = ∞, 30 and 10. (b) Variations of CTAB and Na^+ (external surface), evaluated from chemical analysis, as a function of the alumina content (in Al/(Si + Al)).

$$S = (4.10^4/\rho t)(1 - t/a)/(2 - t/a) \quad (1)$$

where t is the wall-thickness, a the cell parameter, ρ the silica density, and S the surface area.

Equation 1 for large-pore MTS (with $t/a \ll 1$) becomes:

$$t\,(\text{Å}) = 9091/S \quad (2)$$

This calculation showed that the wall thickness decreased from 11 to 9 Å by adding alumina from Si/Al = ∞ to Si/Al = 60. This texture variation is a consequence of the repulsion of the hydrophobic TMB played by the surface negatively charged aluminosilicate species. Therefore, TMB was partially impeded to promote silica condensation. Indeed, previous studies about the surface properties of pure silica large-pore MTS (by adding TMB to the synthesis mixture containing pure silica)[28,29] showed an increase of the MTS surface hydrophobicity due to the localization of TMB in vicinity of the micelle surface during the synthesis: hydrophobic siloxane sites were formed at the surface by means of condensation of silica in the vicinity of TMB. Therefore, TMB influences the surface properties of MTS materials. But in the presence of alumina at Si/Al = 60, it was partially repulsed by the charged surface groups, giving rise to a lower silica condensation. This, in turn, will contribute to form a thinner wall and therefore to increase the surface area of the materials (see eqs 1−2). Furthermore, the small alumina content at Si/Al = 60 slightly perturbed the swelling effect of TMB by decreasing the amount of TMB incorporated in the micelles because less TMB localized at the interface: the interface was less hydrophobic, so it was less favorable to TMB incorporation. The pore size was then consequently reduced.

From Si/Al = 60 to 10, the variation of surface area was inverted (Table 1), showing a decrease from 987 to 826 m^2/g, which corresponds to an increase of wall thickness from 9 to 11 Å. This is explained on the basis of the increase in the amount of Na^+ cations incorporated in the solid, as evaluated by means of chemical analysis and shown in Figure 1b as a function of the Al content: the concentration of Na^+ cations (per SiO_4) increased from 0.006 to 0.027 by decreasing Si/Al from 60 to 10. The presence of Na^+ in the large-pore MTSA came from the cation−π interactions between Na^+ and TMB; these interactions were stronger than the TMB/NH_4^+ interactions because the quaternary ammonium is a softer cation. Evidence of cation−π interactions between Na^+ and TMB also stem from previous studies,[30] which show that, in the absence of TMB, Na^+ is almost absent. Because salts are known to favor silica

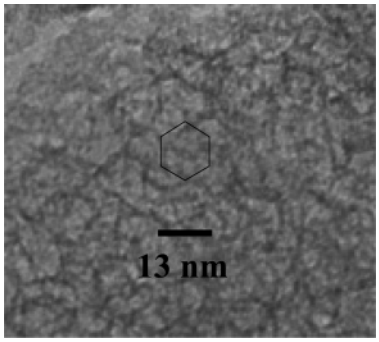

Figure 2. Transmission electron micrograph (TEM) of the calcined MTSA obtained with TMB/CTAB = 13 and Si/Al = 60.

condensation, increasing amounts of Na^+ at the MTSA surface increase the wall thickness, which is responsible for decreasing the surface area and the pore volume.

An increase in pore size (from 76 to 96 Å) is observed for MTSA from Si/Al = 30 to Si/Al = 10 (Table 1), resulting from an improved swelling effect of TMB, which was no more repulsed by the surface: at these alumina contents, the negatively charged alumina groups were neutralized by the positively charged cetyltrimethylammonium (CTMA) groups of CTAB. This result was confirmed by inspecting the variation of the CTAB amount, obtained from chemical analysis, as a function of the alumina content (Al/(Si + Al)), also reported in Figure 1b. Indeed, from Si/Al = 60 to Si/Al = 10, the CTAB content decreased, although all CTAB was incorporated in the large-pore MTSA (CTAB yield of about 100%, reported in Table 1). This means that the CTMA head was used to neutralize the aluminate charge at the solid surface. Therefore, the graphs in Figure 1b show that, from Si/Al = 60 to Si/Al = 10, both CTMA and Na^+ were engaged to neutralize the negatively charged surface groups, but the Na^+ ions were also involved in the cation$-\pi$ interactions with TMB. Therefore, CTMA wins the competition with Na^+ for neutralizing the surface charged sites.

Then at the highest Al content (Si/Al < 10), in correspondence with the drop in CTMA yield, the Na^+ amount increased. These higher amounts of alumina (Si/Al < 10) created a heterogeneous, partly amorphous structure that needed the Na^+ cations for the surface charge compensation and poorly interacted with CTMA, which was, therefore, almost not used in the formation of the amorphous material. The data in Table 1 show that Na^+ cations incorporated in these structures were no longer totally exchangeable by NH_4^+ (an almost complete exchange was found at Si/Al ≥ 10). Half of the Na^+ cations were entrapped into the walls of the new amorphous structure. As for MTSA synthesized without TMB,[30] the incorporation of Na^+ cations in the solid was a source of disorganization: some aluminate groups were not compensated by CTMA (CTMA/Al < 1), and material reorganization occured. At Si/Al = 7, the demixing of the synthesis mixture favored the formation of a double porosity, with pore diameters of 90 and 35 Å (Table 1), corresponding to a TMB-rich fraction, which provided the large-pore MTSA and a TMB-poor fraction, giving rise to the narrow pore MTSA. We also tried higher amounts of CTAB in the synthesis, up to CTAB/SiO_2 = 0.57, but even if the relative amount of small pores diminished, we did not obtain a single large-pore MTSA.

For Si/Al = 6, only the material with the narrow pores was obtained, characterized by the so-called MCM-41 structure.[1−6]

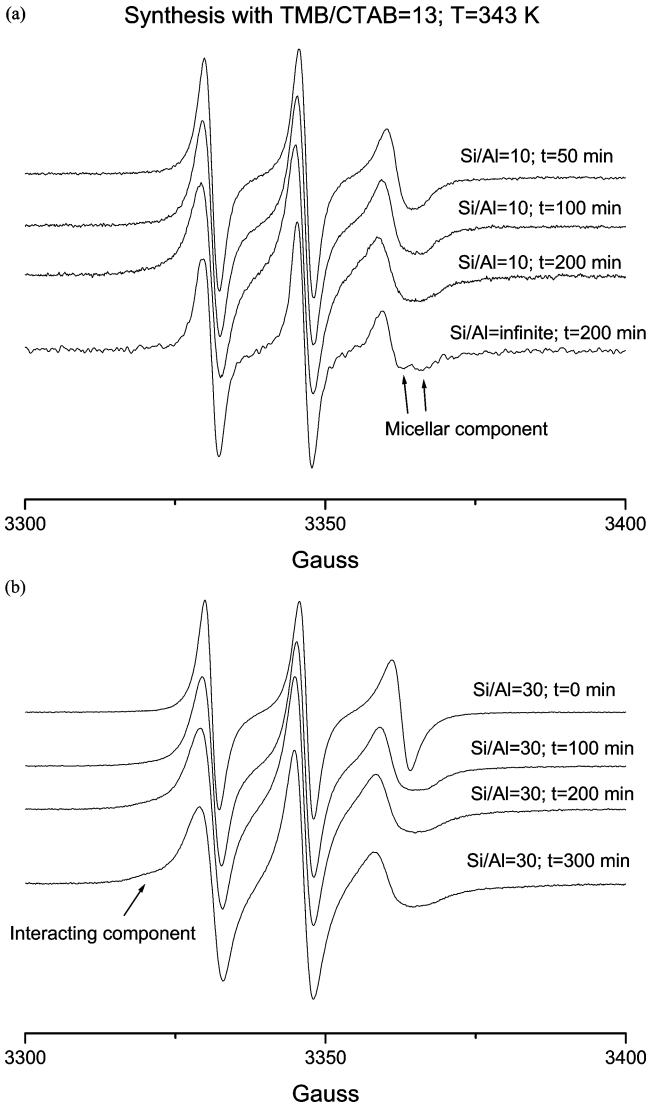

Figure 3. Examples of experimental EPR spectra for the synthesis with TMB/CTAB = 13. (a) Si/Al = ∞ − t = 200 min. Si/Al = 10 − t = 50, 100, 200 min. (b) Si/Al = 30 − t = 0, 100, 200, 300 min. The arrows indicate the main peaks for the micellar and the interacting components.

Finally, for Si/Al = 5, a different structuration of the material took place and the resulting amorphous MTSA featured a pore size of 100 Å with a low surface area of 479 m^2/g (Table 1).

The main result is that, for both as-synthesized and calcined large-pore MTSA in the presence of TMB (at TMB/CTAB = 13), a frontier was found at Si/Al = 10. Indeed, the large-pore MTSA obtained at Si/Al < 10 was less stable than the material synthesized with a lower alumina content (Si/Al ≥ 10), which led to a more homogeneous material and increased the amount of TMB incorporation in the CTAB aggregates.

As previously shown in MTSA synthesis without TMB,[30] the formation of a hexagonal MTSA structure at high alumina contents competed with the formation of an amorphous MTSA. Without TMB, the frontier was found at Si/Al = 15. TMB allowed incorporation in the hexagonal solid structure of a higher amount of alumina without forming amorphous side product, and the frontier between a completely hexagonal MTSA and a mixed hexagonal + amorphous MTSA was shifted from Si/Al = 15 to Si/Al = 10.

Furthermore, in the absence of TMB, no change in surface area and in the volume and pore diameter resulted in the entire

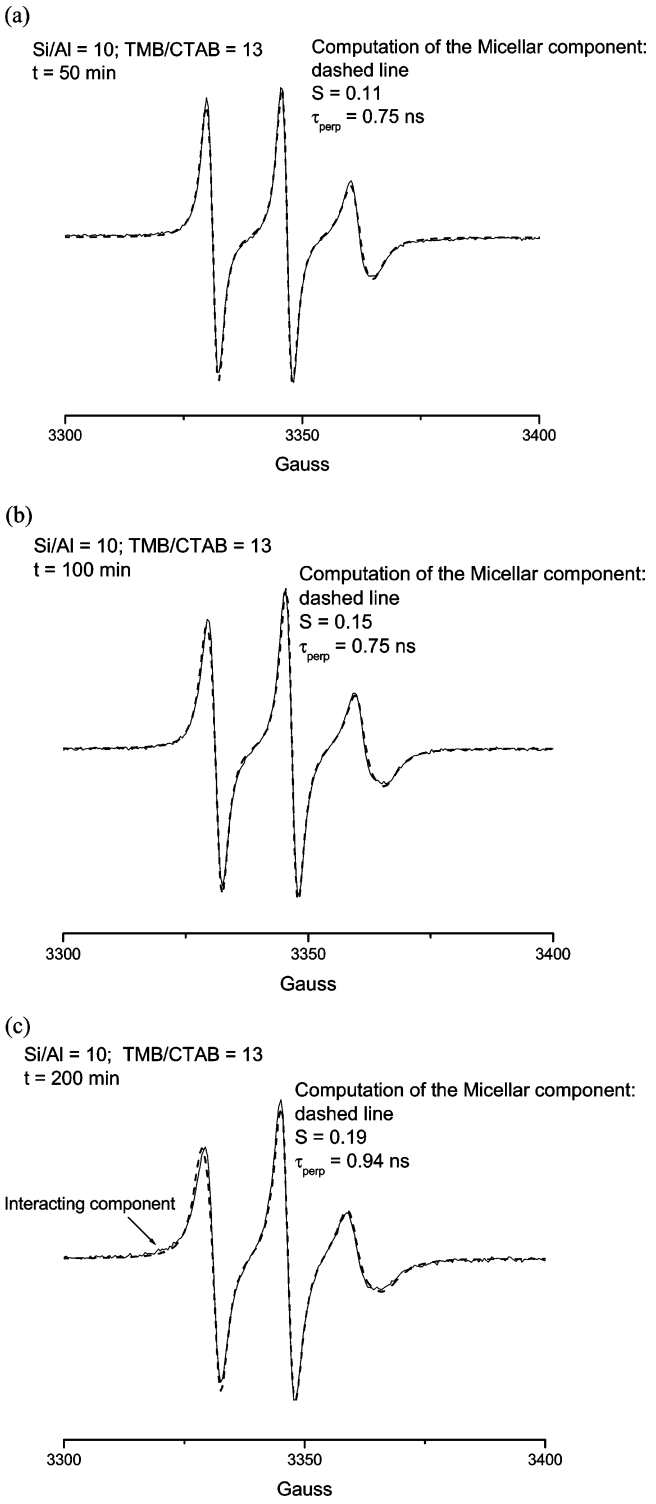

Figure 4. Examples of experimental (full lines) and computed (dashed lines) EPR spectra for the synthesis with TMB/CTAB = 13 (the main parameters used for computation are reported in the figure): (a) Si/Al = 10 and t = 50 min. (b) Si/Al = 10 and t = 100 min. (c) Si/Al = 10 and t = 200 min.

range of Si/Al from ∞ to 15.[30] Therefore, the structure of the solid synthesized using TMB was more affected by the addition of alumina with respect to the solid obtained without TMB.

On the other hand, in the range 5 < Si/Al < 60, it has been found by means of Al MAS NMR that alumina was totally incorporated in tetrahedral form under Si−O−Al species in the solids: a single peak at 52−55 ppm remained after calcination.[27] Also, FTIR measurements (results not shown) support this finding, showing a linear decrease of the symmetric band at 800 cm^{-1} and the asymmetric band at 1000 cm^{-1} when the alumina content increased.

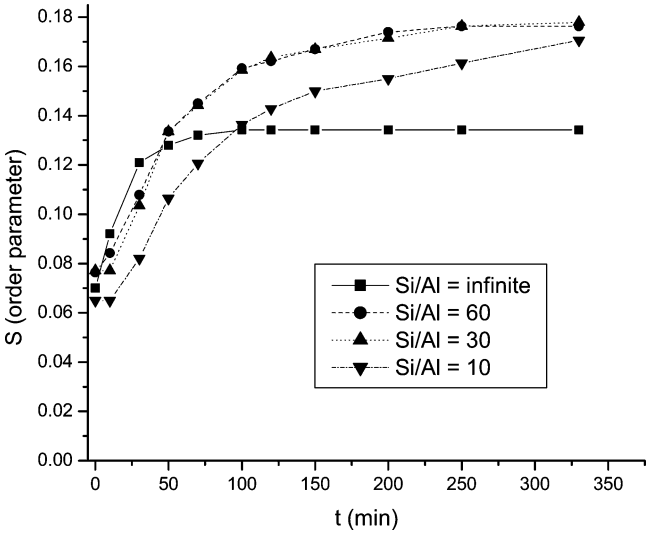

Figure 5. Variation of the order parameter (S) of the micellar component as a function of time for the synthesis with TMB/CTAB = 13 at Si/Al = ∞, 60, 30, 10.

Figure 2 shows the transmission electron micrograph (TEM) of the calcined MTSA obtained with TMB/CTAB = 13 and Si/Al = 60. However, the TEM images at different Si/Al, down to Si/Al = 10, look very similar to each other, characterized by homogeneous large pores with very thin walls (around 10 Å) among them. In this case, the pore is not clearly identified and tentatively sketched in the figure with a hexagon.

As described in the next section, the EPR results are in perfect accordance with the results described in this section.

EPR Analysis. For the EPR experiments, only the domain of large-pore MTSA formation, that is, Si/Al from ∞ to 10, provided reliable and trustworthy results. Experiments conducted at Si/Al < 10 (synthesis at Si/Al = 7 and 5 were tested) did not provide reproducible results due to a separation of the material in different phases in the EPR tube since the beginning of the synthesis, that is, a demixing of the synthesis mixture. This is in agreement with the formation of a heteroporous material and at least a fraction of amorphous material, as found by means of the surface characterization. Conversely, the results from synthesis mixtures at Si/Al ≥ 10 provided reproducible and reliable results, as discussed in the following.

Figure 3 shows selected spectra for the synthesis in the presence of TMB at different Si/Al ratios. Figure 3a: Si/Al = ∞ − t = 200 min. Si/Al = 10 − t = 50, 100, 200 min. Figure 3b: Si/Al = 30 − t = 0, 100, 200, 300 min. The two peaks indicated with two arrows as the micellar component in Figure 3a may be separately computed, as shown in a previous study,[28] as a "fast component" (left peak), with τ_{perp} = 0.17 ns, and a "slow component" (right peak), with τ_{perp} = 1 ns. In this study, this micellar component was adequately computed for all the spectral series in the presence of alumina at the different Si/Al ratios by including in the line shape calculation the so-called order parameter, S. This last parameter arose when the probes were inserted in a layerlike structure of surfactants and felt the ordering of the environmental surfactants, forming a "palisade" (S = 0, no order; S = 1, complete ordering). Actually, this happened in the presence of TMB that swelled the surfactant aggregates and therefore enlarged the pore size. In this case, the pore wall became a flat surface where the surfactants self-organized in an ordered layer. Therefore, TMB provoked the

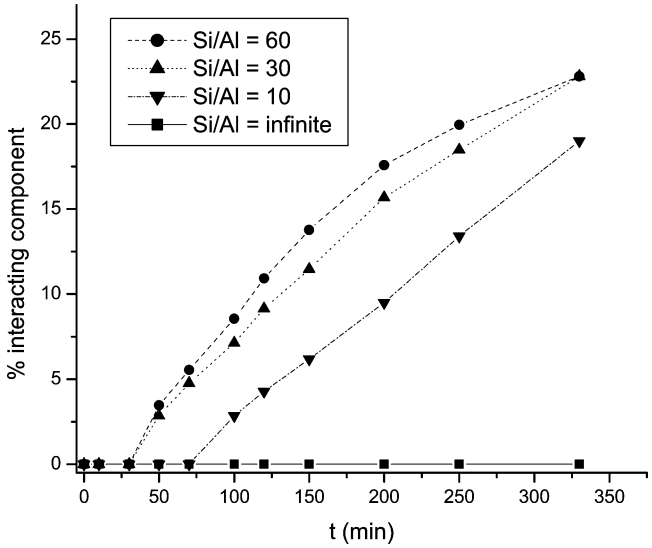

Figure 6. Variation of the percentage of the interacting component as a function of time for the synthesis with TMB/CTAB = 13 at Si/Al = ∞, 60, 30, 10.

structuration of the surfactants, at the sides of the large pores, in a partially ordered configuration where the radical groups (belonging to the radical surfactant head) inserted in the chain layer in the vicinity of the surfactant heads: only this location justifies that the NO group, even if belonging to the radical-surfactant head, monitors the chain ordering.

Parts a−c of Figure 4 provide examples of the computations of the EPR signals for the synthesis with Si/Al = 10, at t = 50, 100, and 200 min, respectively. The main input parameters used for the computation (S and τ_{perp}) are also reported in the figures. The longer the synthesis times, the higher the S value, indicating the progressive structuration of the surfactants over time in a layerlike structure.

Computation of the micellar component was performed at different Si/Al ratios and synthesis times. This analysis provided the order parameter plotted in Figure 5 as a function of the synthesis time for selected Si/Al ratios, that is ∞, 60, 30, and 10. In the absence of alumina (Si/Al = ∞), a quick increase of S occured, which is complete after 50 min of synthesis. Conversely, increasing amounts of alumina provoked a delay in the structuration of the ordered layer: the order parameter started contributing after some minutes of synthesis and then the increase of S was slowed by the increasing amounts of alumina. At Si/Al = 10, S was still increasing after 400 min of synthesis, indicating that the structure of the aggregates was still changing.

Therefore, the information, extracted from the analysis of the graphs in Figure 5, are to some extent similar to those obtained for the synthesis in the absence of TMB,[30] which indicated that alumina, added to silica, promoted but slowed down the structuration of the surfactant aggregates and, consequently, of the solid; for instance, the larger the amount of alumina, the smaller the slope for the increase of S over time, that is, the later the time at which the layerlike structure was formed. Accordingly, with this delay effect, in the first minutes of synthesis, S increased by increasing Si/Al in the sequence 10 < 30 < 60 < ∞ (the larger the Al amount, the lower the "initial" order). But at the end of the synthesis, this sequence is completely reversed, that is, ∞ < 60 < 30 < 10 (the larger the Al amount, the higher the "final" order). Therefore, the final ordering was enhanced by increasing alumina contents. In accordance with the results from MTSA characterization in the

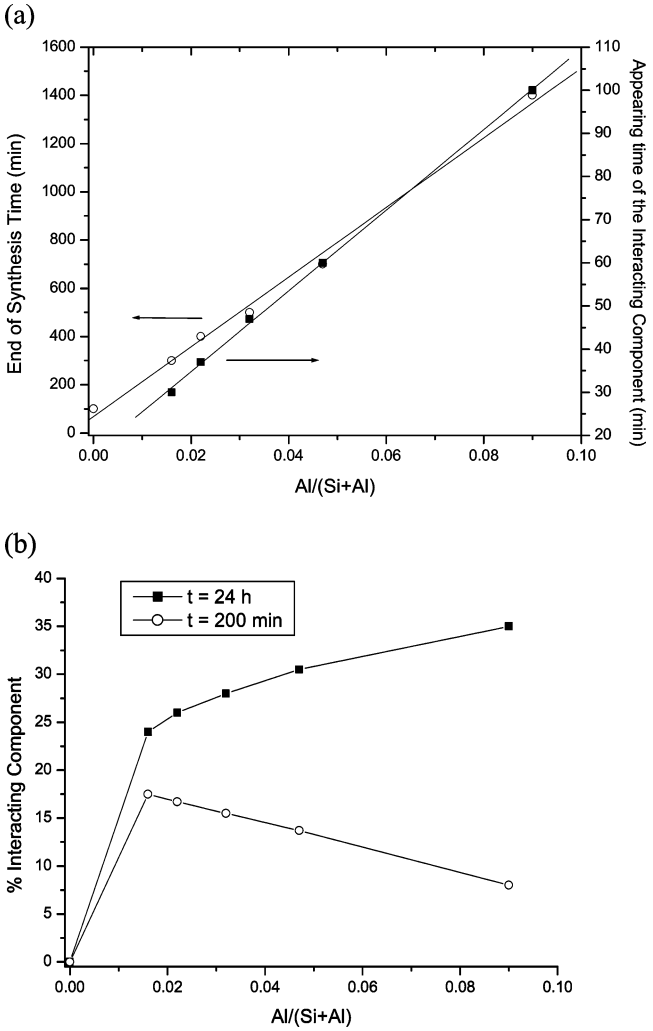

Figure 7. (a) Appearing time of the interacting component (right axis), and ending time of the synthesis (left axis), as a function of the alumina content (Al/(Si + Al)); (b) percentage of the interacting component as a function of the Al content (Al/(Si + Al)) for the synthesis times t = 200 min and t = 24 h.

previous section, the final ordering of the surfactant layer was correlated with the amount of Na^+ cations present at the surfactant/solid interface, which slowed the organization of the surfactant by competing with the surfactant heads to neutralize the charged surface groups, and this effect slowed down the ordering of the surfactant and the final condensation of the solid. However, as discussed above, the surfactant heads win this competition because Na^+ is also engaged with TMB by means of cation−π interactions.

This means that the ordering effect was improved by replacing the siloxane Si−O−Si groups with charged Si−O^-−Al at the surface of the pores. As previously found, siloxanes groups resulted from the condensation of silanols due to the presence of TMB in vicinity of the surface.[28] Conversely, the charged MTSA surface repulsed the hydrophobic TMB molecules. A different distribution of TMB and the enhanced interactions of the surfactant heads with the oppositely charged surface groups favored the formation of the ordered layer at the higher alumina contents.

In the synthesis in the absence of TMB,[30] the EPR analysis showed that a high amount of alumina corresponding to Si/Al = 10 impeded both the organization of the surfactants and the consequent formation of a hexagonal MTSA structure. In the presence of TMB, as demonstrated by means of the sorption

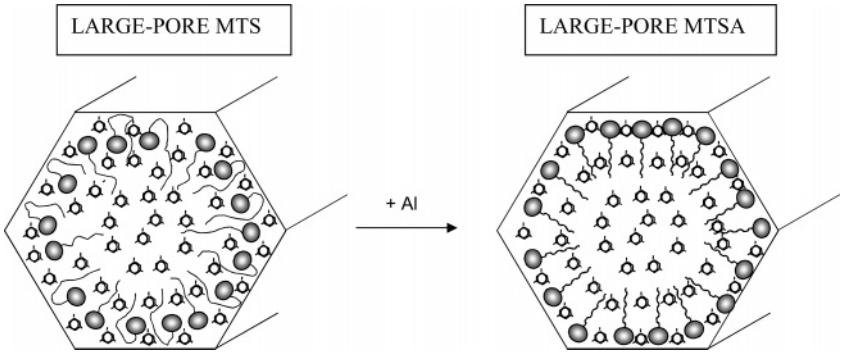

Figure 8. Scheme for the distribution and organization of the surfactants and TMB in the pores of as-synthesized large-pore MTS (without alumina) and large-pore MTSA (with alumina).

isotherms, only at Si/Al < 10 a demixing of the synthesis mixture occurred and then an amorphous material started forming. The EPR results are in agreement with these results and indicate that, even at Si/Al = 10, the TMB/CTAB = 13 mixture formed an ordered structure that leads to the formation of a large-pore hexagonal MTSA solid. This high amount of alumina (Si/Al = 10) only slowed down the kinetics of the synthesis. In this condition, the large sides of the wide pores easily hosted the aluminate groups, whereas strong structural distortions occured in the narrow-pore MTSA in the absence of TMB, which led to destructuration of the solid itself.

Indeed, previous studies[27] show that the hydrophilic sites are usually localized at the sides of the pores, whereas the hydrophobic sites preferentially locate in the pore corners; in line with this finding, the large sides of the pore wells organized the hydrophilic aluminate groups, even in the presence of TMB, which already demonstrated increasing of the hydrophobicity of the pore sides of MTS.[28] When alumina is present, the hydrophobic Si−O−Si on the pore sides is replaced by the anionic Si−O$^-$−Al, which partially repulses and redistributes the TMB molecules, favoring the stabilization of an ordered surfactant layer at the surface of the homoporous MTSA even at Si/Al = 10.

The spectra obtained by increasing the synthesis time, in the presence of alumina, could not be correctly computed by means of the micellar component alone (as for the synthesis of large-pore MTS without alumina)[28] because, as indicated with an arrow in Figure 3c, the interacting component also contributes to the overall EPR signal. Therefore, to improve the fitting between the experimental and the computed spectra, it is necessary to add the two computed components, the micellar and the interacting ones, at the proper relative percentages of the two components.

It is noteworthy that this interacting component, not present in the absence of alumina, appeared when alumina was added to the synthesis mixture of large-pore MTS using TMB: the replacement of siloxane (Si−O−Si) by the charged Si−O$^-$−Al at the pore sides is responsible of the electrostatic interactions between the negatively charged silicoaluminate groups and the positively charged surfactant heads, giving rise to the interacting component. Therefore, in the absence of alumina and in the presence of TMB, the silanol groups did not originate strong interactions with the surfactant heads because of the cation−π interactions between TMB and CTMA, whereas an interacting component arising from the silanol−CAT16 interactions was found for MTS synthesis using no TMB.[26] This in turn further supports the conclusion that the silicoaluminate groups repulse TMB, which, in the absence of alumina, localized in the vicinity of the aggregate surface[28] and promoted the condensation of silanols to form hydrophobic siloxane groups at the MTS surface, thus impeding strong electrostatic interactions.

The computation of the spectra provided the percentage of the interacting component, which therefore worked as a measure of the structuration of the pore side walls where the Si−O− Al localized and, consequently, of the large-pore MTSA materials. The variation of this percentage as a function of the synthesis time, shown in Figure 6, provided the following information about the kinetics of solid formation and the surface properties: (1) The "appearance" of the interacting component (consider that the interacting component becomes detectable when the % ≥ 2.5) is delayed by increasing amounts of alumina. Figure 7a (right axis) shows the variation of the appearing time of the interacting component as a function of the alumina content (as Al/(Si + Al)). This graph evidences the perturbing affect of alumina in the solid structuration because the appearing time is delayed proportionally to the alumina content. (2) As shown in Figure 6, the percentage of the interacting component increases over time until a plateau is reached. The invariance of the relative amount of the interacting component nicely works as an indicator of the end of the synthesis. Also, this ending time of the synthesis is delayed proportionally to the alumina content. This is also demonstrated by the linear variation of the end of synthesis time as a funcion of Al/(Si + Al) in Figure 7a (left axis). The graphs in Figure 7 therefore indicate that condensation and structuration of silicoalumina materials to form large-pore hexagonal structures is linearly delayed by the increase in the alumina contents due to the substitution of the silanols with the charged silicoaluminate groups. (3) Figure 7b shows the variation of the percentage of the interacting component as a function of the Al content for two synthesis times: t = 200 min and t = 24 h. At t = 200 min, the percentage linearly decreased from Si/Al = 60 to Si/Al = 10. This is because of the delay in MTSA structuration played by alumina: the higher the alumina content, the stronger the perturbation in the solid condensation. At t = 24 h, the hexagonal structure is formed at any Si/Al ratio, and therefore what prevails is the increasing amount of silicoaluminate groups at the MTSA surface: the higher the alumina content, the higher the amount of negatively charged silicoaluminate sites that interact with the positively charged surfactant heads.

Conclusions

The addition of TMB as a swelling agent of the CTAB aggregates at TMB/CTAB = 13 produced large-pore homogeneous and stable MTSA materials in the Si/Al range from ∞ to 10, as found by nitrogen adsorption−desorption isotherms: the pore size varied between 92 and 110 Å. In this Si/Al range, a hexagonal MTSA structure was obtained, characterized by thin

walls, as also demonstrated by SEM micrographs. At lower Si/Al ratios (Si/Al < 10), a double porosity and, eventually, an amorphous structure, were formed due to the demixing of the synthesis mixture. In these conditions, the EPR results, obtained by introducing the surfactant CAT16 probe in the CTAB aggregates, were not reproducible. At Si/Al ≥ 10, TMB introduced in the synthesis mixture leads to the formation of a layerlike structure of the surfactants, which requires the introduction of an order parameter in the EPR spectral computation. In the absence of alumina, TMB localizes in vicinity of the silanol groups at the surface, whereas, in the presence of alumina, the hydrophobic Si−O−Si groups on the pore sides are replaced by the anionic Si−O^-−Al groups, which partially repulse TMB molecules at the solid/micelle interface and are also responsible for stronger interactions between the surfactants and the solid surface, which give rise to an interacting component contributing to the EPR line shape. The cation−π interactions between Na^+ and TMB limit the negative effect of Na^+ cations on MTSA structuration observed for synthesis without TMB at Si/Al = 10.

Figure 8 shows the proposed scheme for the different organization of the surfactants and TMB in the large-pores of MTSA in the absence and in the presence of alumina: in the absence of alumina, the low polar Si−O−Si groups, formed at the surface due to the presence of TMB, favor the hydrophobic interactions with the surfactant chains, which consequently form a less-ordered layer and weak interactions. Conversely, in the presence of both TMB and alumina, the CTAB surfactants form an ordered layer at the large pore sides. Part of the radical surfactant heads are inserted in the ordered layer, thus monitoring the ordered structure, and part of these CAT16 heads are directly interacting with the silicoaluminate groups, giving rise to the interacting component. Therefore, the EPR analysis of CAT16 inserted in the synthesis mixture well monitors both the assembly or ordering of the surfactants and the solid condensation and structuration, providing information on the synthesis kinetics and the MTSA organization.

Acknowledgment. We thank Christine Biolley for the great help in the MTSA synthesis. We thank Claudia Mariani, Roberto Mazzeo, Daniele Sabbatini, Ivano Calzolari, and Lucio Falasca for the help in the EPR analysis.

References and Notes

(1) Kresge, C. T.; Leonowicz, M. E.; Roth, W. J.; Vartuli, J. C.; Beck, J. S. *Nature* **1992,** *359*, 710.

(2) Beck, J. S.; Vartuli, J. C.; Roth, W. L.; Leonowicz, M. E.; Kresge, C. T.; Schmidt, K. D.; Chu, C. T.-W.; Olson, D. H.; Sheppard, E. W.; McCullen, S. B.; Higgins, J. B.; Schenkler, J. L. *J. Am. Chem. Soc.* **1992,** *114*, 10834.

(3) Inagaki, S.; Fukushima, Y.; Kuroda, K., *J. Chem. Soc., Chem. Commun.* **1993**, 680.

(4) (a) Huo, Q.; Margolese, D. I.; Ciesla, U.; Feng, P.; Gier, T. E.; Sieger, P.; Leon, R.; Petroff, P. M.; Schüth, F.; Stucky, G. D. *Nature* **1994** *368,* 317. (b) Huo, Q.; Margolese, D. I.; Ciesla, U.; Demuth, D. G.; Feng, P.; Gier, T. E.; Sieger, P.; Firouzi, A.; Chmelka, B. F.; Schüth, F.; Stucky, G. D. *Chem. Mater.* **1994,** *6*, 1176.

(5) Tanev, P. T.; Pinnavaia, T. J. *Science* **1995**, *271,* 1267.

(6) Bagshaw, S. A.; Prouzet, E.; Pinnavaia, T. J., *Science* **1995**, *269,* 1242.

(7) Armengol, E.; Cano, M. L.; Corma, A.; Garcia, H.; Navarro, M. Y. *J. Chem. Soc., Chem. Commun.* **1995**, 519.

(8) (a) Corma, A.; Martinez, A.; Martinez-Soria, V.; Monton, J. B. *J. Catal.* **1995**, *153,* 25. (b) Corma, A.; Navarro, M. T.; Pariente, J. P. *J. Chem. Soc., Chem. Commun.* **1994,** 147.

(9) Tanev, P. T.; Chibwe, M.; Pinnavaia, T. J. *Nature* **1994,** *368*, 321.

(10) Wu, C. G.; Bein, T. *Science* **1994,** *264*, 1757.

(11) Llewellyn, P. L.; Ciesla, U.; Decher, H.; Stadler, R.; Schüth, F.; Unger, K. *Stud. Surf. Sci. Catal.* **1994,** *84*, 2013.

(12) Branton, P. J.; Hall, P. G.; Sing, K. S. W.; Reichert, H.; Schüth F.; Unger, K. *J. Chem. Soc., Faraday Trans.* **1994,** *90*, 2821.

(13) Schmidt, R.; Stöcker, M.; Hansen, E.; Akporiaye, D.; Ellestad, O. H. *Microporous Mater.* **1995,** *3*, 443.

(14) Ying, J. Y.; Mehnert, C. P.; Wong, M. S. *Angew Chem., Int. Ed.* **1999**, *38*, 56.

(15) Patarin, J.; Lebeau, B.; Zana, R. *Curr. Opin. Colloid Interface Sci.* **2002**, *7*, 107.

(16) (a) Chen, C. Y.; Li, H.-X.; Davis, M. E. *Microporous Mater.* **1993,** *2*, 17. (b) Chen, C. Y.; Burkett, S. L.; Li, H.-X.; Davis, M. E. *Microporous Mater.* **1993,** *2*, 27.

(17) Vartuli, J. C.; Schmidt, K. D.; Kresge, C. T.; Roth, W. J.; Leonowicz, M. E.; McCullen, S. B.; Hellring, S. D.; Beck, J. S.; Schenkler, J. L.; Olson, D. H.; Sheppard, E. W. *Chem. Mater.* **1994,** *6*, 2317.

(18) Fyfe, C. A.; Fu, G. *J. Am. Chem. Soc.* **1995,** *117,* 9709.

(19) Firouzi, A.; Kumar, D.; Bull, L. M.; Bessier, T.; Sieger, P.; Huo, Q.; Walker, S. A.; Zasadinski, J. A.; Glinka, C.; Nicol, J.; Margolese, D.; Stucky, G. D.; Chmelka, B. F. *Science* **1995**, *267,* 1138.

(20) Monnier, A.; Schüth, F.; Huo, Q.; Kumar, D.; Margolese, D.; Maxwell, R. S.; Stucky, G. D.; Krishnamamurty, M.; Petroff, P.; Firouzi, A.; Janzationicke, M.; Chmelka, B. F. *Science* **1993**, *1261,* 1299.

(21) Regev, O. *Langmuir* **1996**, *12*, 4940.

(22) Zholobenko, V. L.; Holmes, S. M.; Cundy, C. S.; Dwyer, J. *Microporous Mater.* **1997,** *11*, 83.

(23) Ortlam, A.; Rathousky, J.; Schulz-Ekloff, G.; Zukal, A. *Microporous Mater.* 1996, *6,* 171.

(24) Zhang, J.; Luz, Z.; Goldfarb, D. *J. Phys. Chem. B* **1997**, *101*, 7087.

(25) Zang, J.; Carl, P. J.; Zimmermann, H.; Goldfarb, D. *J. Phys. Chem.* **2002**, *106*, 5382

(26) Galarneau, A.; Di Renzo, F.; Fajula, F.; Mollo, L.; Fubini, F.; Ottaviani, M. F. *J. Colloid Interface Sci.* **1998**, *201*, 105.

(27) Ottaviani, M. F.; Galarneau, A.; Desplandier-Giscard, D.; Di Renzo, F.; Fajula, F. *Microporous Mesoporous Mater.* **2001**, *44*, 1, (nTAB-MTSA).

(28) Ottaviani, M. F., Moscatelli, A.; Desplandier-Giscard, D.; Di Renzo, F.; Kooyman, P. J.; Alonso, B.; Galarneau, A. *J. Phys. Chem. B* **2004**, *108*, 12123.

(29) Moscatelli, A.; Galarneau, A.; Di Renzo, F.; Ottaviani, M. F. *J. Phys. Chem. B* **2004**, *108*, 18580.

(30) Galarneau, A.; Cangiotti, M.; Di Renzo, F.; Fajula, F.; Ottaviani, M. F. *J. Phys. Chem. B* **2006**, *110*, 4058.

(31) (a) Schneider, D. J.; Freed, J. H. In *Biological Magnetic Resonance. Spin Labeling. Theory and Applications*; Berliner, L. J., Reuben, J., Eds.; Plenum Press: New York, 1989, Vol. 8, p 1. (b) Budil, D. E.; Lee, S.; Saxena, S.; Freed, J. H. *J. Magn. Res., Ser. A* **1996**, *120*, 155.

(32) Broekhoff, J. C. P.; De Boer, J. H. *J. Catal.* **1968,** *10*, 377.

(33) Galarneau, A.; Desplantier, D.; Dutartre, R.; Di Renzo, F. *Microporous Mesoporous Mater.* **1999**, 27, 297.

(34) Galarneau, A.; Desplantier-Giscard, D.; Di Renzo, F.; Fajula, F. *Catal. Today* **2001**, *68*, 191.